Tech Science Press

An Adaptive SAR Despeckling Method Using Cuckoo Search Algorithm

Memoona Malik[*], Iftikhar Azim, Amir Hanif Dar and Sohail Asghar

COMSATS University Islamabad, Islamabad, 44000, Pakistan
[*]Corresponding Author: Memoona Malik. Email: memoonamalik@comsats.edu.pk

Abstract: Despeckling of SAR imagery is a crucial step prior to their automated interpretation as information extraction from noisy images is a challenging task. Though a huge despeckling literature exists in this regard, there is still a room for improvement in existing techniques. The contemporary despeckling techniques adversely affect image edges during the noise reduction process and are thus responsible for losing the significant image features. Therefore, to preserve important features during the speckle reduction process, a two phase hybrid despeckling filter is proposed in this study. The first phase of the hybrid filter focuses on edge preservation by employing a new edge detection criterion for the guided filter. Whereas the second phase attempted to suppress speckle by utilizing some speckle suppression and edge preservation filters whose sequence is determined by the cuckoo search optimization algorithm (CSO). The CSO generates optimal sequences of these filters according to the nature of input images with peak signal-to-noise ratio (PSNR) and structural similarity index (SSIM) as its objective function. Performance comparison of the proposed hybrid filter with state-of-the art techniques has revealed its best despeckling behavior on standard and real SAR images.

Keywords: Cuckoo search optimization; edge preserving filters; hybrid filter; noise suppressing filters; SAR despeckling; speckle noise

1 Introduction

SAR (Synthetic Aperture Radar) imaging systems have been extensively used in Earth monitoring satellites for surveillance purposes as they provide high resolution images in the presence of natural obstacles such as clouds, dust, snow and drizzle [1]. However, due to the occurrence of speckle noise in SAR imagery, automated interpretation of these images becomes difficult. Usually speckle noise induces strong random variations in digital images due to its multiplicative nature. Therefore, it is responsible for severe distortion of important image contents in both homogeneous and heterogeneous regions (such as edges and textures) [2].To resolve this problem, many despeckling techniques have been developed so far which can be broadly classified into hybrid and non-hybrid techniques. The non-hybrid techniques are further classified into spatial domain filters i.e., local and non-local (NL), and frequency domain filters such as wavelets and curvelets.

The concept of local filters did not work well for heterogeneous regions as values of the neighboring pixels are quite different from the value of the pixel to be altered. Thus, local filters do not remove noise in heterogeneous regions and are responsible for blurring textures and edges due to the wrong estimation [3,4]. To overcome the problem of local filters, researchers have devised NL filters in past few years. Unlike local filters, these filters look up for a similar pixel or a block anywhere in the image which exhibits the same statistical nature as that of the selected pixel to preserve images' fine details. However, all the NL based approaches suffer from the issues of increased computational cost, over-smoothening of low contrast regions and blurring of fine details at higher noise intensities while leaving residuals near the edges [5,6].

The wavelet based methods have also been extensively utilized for noise reduction purposes. But, the wavelet representation of 2D images produces a large number of wavelet coefficients that needs to be estimated for noise reduction. Estimating a large number of coefficients results in high mean square errors which affects the despeckling accuracy of wavelets [7]. Moreover, the wavelet transform based approaches are responsible for producing Gibbs-like ringing effects in homogeneous regions and near the edges [8]. In contrast, the curvelet transform is a better noise reduction scheme which is designed using mutilscale ridgelets at very fine scales to represent the curved edges as straight lines. This property of curvelet transform help preserve edges in a noisy image [9–11]. However, they fail to smooth homogeneous areas.

To cater all the above discussed issues of individual filters, various hybrid filters were proposed to reduce the speckle and preserve image details simultaneously [12–22]. Some of the hybrid filters investigated the parallel combination of existing filters i.e. SAR-BM3D and HLSS-C. These type of parallel combinations are computationally complex as the constituent filters itself belong to the category of hybrid ones. In contrast, those hybrid filters which has explored the sequence of standalone filters i.e. wiener filter, wavelet transform, cosine transform, guided filter, weighted least square filters, accomplishes the better despeckling performance with reasonable cost. For instance, SAR-BM3D, a renowned hybrid filter, has explored the denoising capabilities of wiener filtering in the wavelet transformed domain. Cost of SAR-BM3D is far less than the above described parallel combinations. The notion of SAR-BM3D has outperformed all the previous filters in SAR despeckling, however, it suffers from the blurring effect of wiener filtering and incapability of wavelets in edge preservation. Due to these limitations of the employed techniques, SAR-BM3D produces whitish areas in homogeneous regions and undergoes loss of details in heterogeneous regions.

This scenario motivates us in designing a novel despeckling approach that would despeckle different natured images i.e., images rich in homogeneous content and images containing high degree of edges, without losing important image details. Hence, in this paper, a concept of two phase hybrid filter is proposed that would preserve edges in the first phase and despeckle the diverse natured images in the second phase.

For edge preservation, a modified guided filter with a new edge detection criterion is proposed in the first phase. Whereas for speckle reduction, an adaptive sequence of some noise suppressing and edge preserving filters is determined in the second phase. The sequences are in accordance with the varying nature of images. Therefore, the proposed two phase hybrid filter is expected to better suppress noise in different types of images while preserving the significant image features. Detailed explanation of the proposed approach is provided in Section 2 while experimental evaluation of the proposed hybrid filter on standard and real SAR images is provided in Sections 3 and 4. And finally, Section 5 presents the conclusion of this paper.

2 Proposed Method

This study proposes a two phase hybrid filter for edge preservation while suppressing the speckle noise especially form SAR imagery. In the first phase, an improved version of the guided filter with a new edge

detection criterion is presented to preserve edges. Afterwards, the output of the proposed guided filter gets fused with the wiener filter to benefit from the wiener's speckle suppression capabilities as well as to obtain an initial estimate of the despeckled image. Though the output of the first phase competes with several despeckling filters in terms of edge retention, it failed to surpass the hybrid filters in despeckling accuracy. Consequently, the second phase becomes complementary for boosting the speckle reduction capabilities of the first phase. The second phase thus takes the initial despeckled estimate as an input and determines a unique sequence of some noise suppressing and edge preserving filters using the CSO. It is expected that the generated unique sequences are in accordance with the nature of the basic estimate i.e. rich in homogeneous or heterogeneous content, and helpful in improving the despeckling accuracy. Block diagram of the proposed two phase hybrid filter is provided in Fig. 1 for further comprehension.
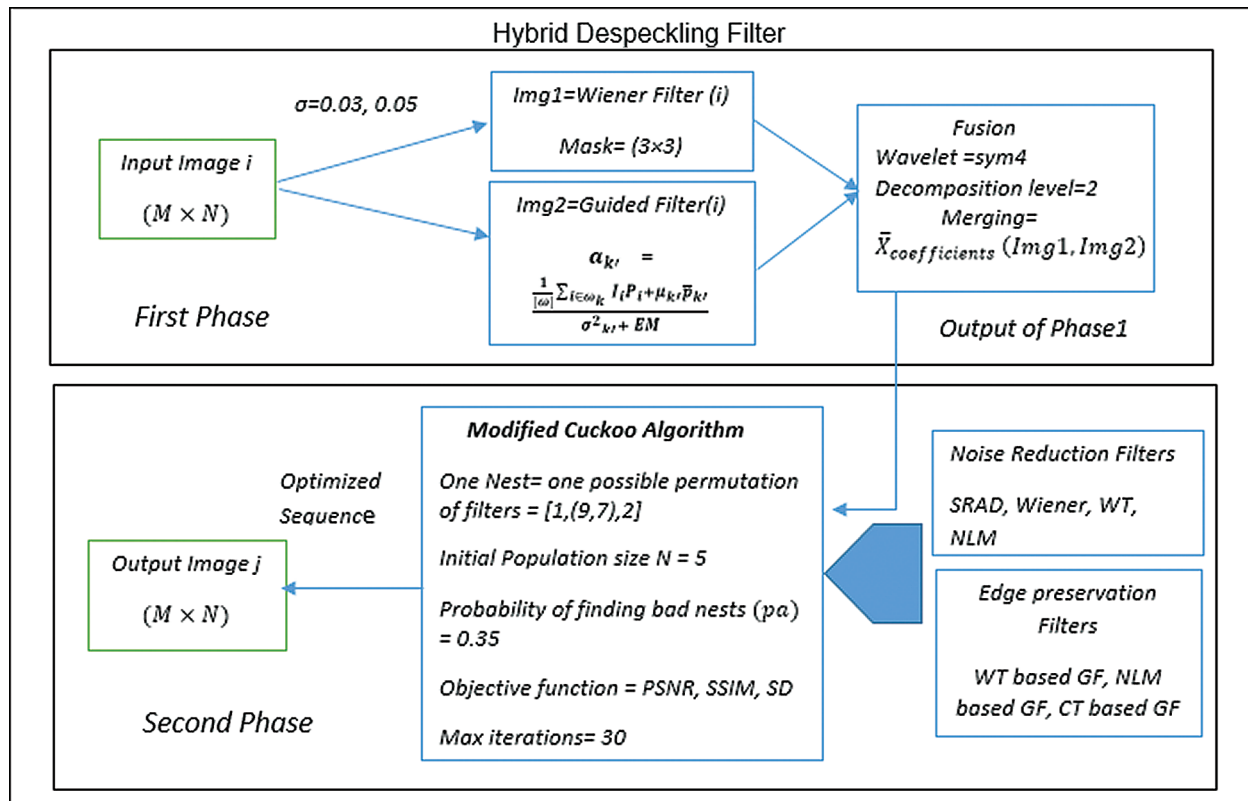

Figure 1: Block diagram of the proposed hybrid filter

2.1 First Phase

The Guided filter was designed with the notion of preserving edges [23]. It performs the neighborhood operation using any guidance image given to it and restores edges by maintaining the edge values as provided in the guidance image. The output of the guided filter, q_i, can be computed as

$$q_i = a_k I_k + b_k, \; \forall i \in \omega_k \tag{1}$$

where I_k is the guidance image, and a_k and b_k are linear coefficients which can be calculated by minimizing the difference between input and the output images.

To improve the edge preserving performance of the guided filter, this study modified the guided filter for speckle suppression by proposing a new edge detection criterion based on the Curvelet transform and the canny edge detection operator.

Among many edge detection operators, canny operator is the one which is considered as the most reliable one. So, we utilized the edge map (EM) generated by the canny operator as a guide to the GF. The EM, being a binary image, restricts the values of a_k to remain in the range of 0 to 1 and provides a reliable edge preserving estimate to the GF. But, the problem associated with the EM is that it is dependent on the input image. If the input image is noisy, then obtaining all the edges may get difficult. Hence, to improve the EM, a curvelet transform is first applied on the noisy input image for speckle reduction. Curvelet transform is a better noise suppression transform than many others with the edge preservation characteristics. It is designed using mutilscale ridgelets at very fine scales to represent the curved edges as straight lines and to preserve them in any noisy image. The canny operator is then applied on the curvelet transformed image to obtain a better EM. The finalized EM is then employed to re-compute the coefficient a_k (Fig. 2).
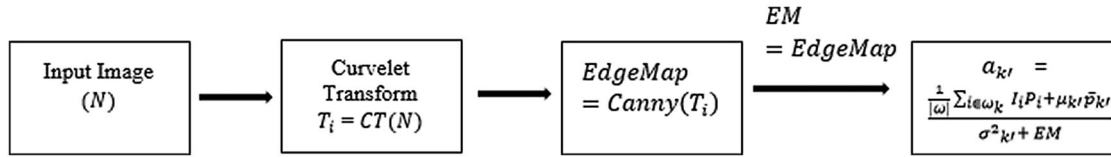

Figure 2: Re-computation of $a_{k'}$ using curvelet transform and canny operator

The proposed *EM* for enhancing the edge preservation performance of the GF can be calculated as:

$$EM = \text{Canny}(T_i) \tag{2}$$

where

$$T_i = CT(N) \tag{3}$$

where *CT* is the curvelet transform and *N* is the input image. To detect edges, this *EM* is incorporated in the Eq. (4) of the GF. The new equation becomes:

$$\text{E}'\left(a_{k'}, b_{k'}\right) = \sum_{i \in w_i} \left((a_k, b_{k'} - p_i) + EM\right) \tag{4}$$

The improved guided filter minimizes the input and output images p_i and q_i. The coefficients a_k and b_k will be recomputed using new edge detection criterion as

$$a_{k'} = \frac{\frac{1}{|\omega|}\sum_{i \in \omega_k} I_i P_i + \mu_{k'}\bar{p}_{k'}}{\sigma^2_{k'} + EM} \tag{5}$$

$$b_{k'} = \bar{p}_{k'} - a_{k'}\mu_{k'} \tag{6}$$

And the output image q_i will then be calculated using $a_{k'}$ and $b_{k'}$ as follows

$$\hat{q}_i = \hat{a}_k I_k + \hat{b}_k \tag{7}$$

where $\hat{a}_k$ and $\hat{b}_k$ represents the mean values of $a_{k'}$ and $b_{k'}$.

Fig. 3 below provides a comparison between GF and the proposed improved GF on fruits image at simulated speckle with variance 0.03 in terms of SSIM. And Fig. 4 presents a comparison between the proposed GF with and without the curvelet transform.
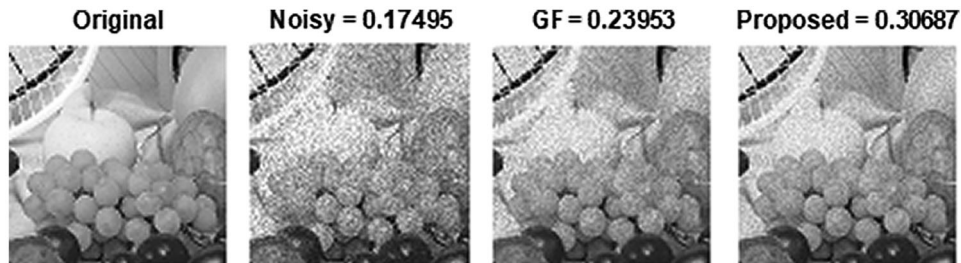

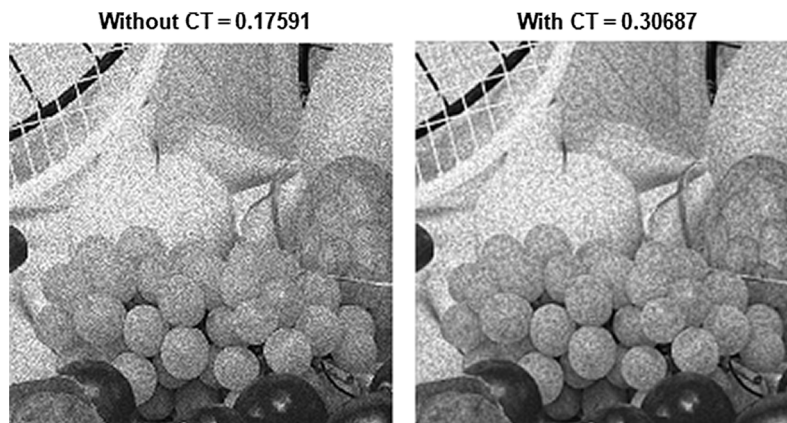**Figure 3:** Comparison of original and improved guided filter

Figure 4: Comparison of proposed guided filter with and without curvelet transform as a guidance image

The curvelet transform is better at edge preservation than speckle suppression. Therefore, the first phase fused the output of the proposed GF with the wiener filter for adequate image smoothing. This fusion combines the edge information provided by the proposed GF with the noise suppressing capability of the wiener filter to produce a despeckled image with preserved edges (Fig. 5).

Figure 5: Performance of filters used in the first phase

Hence, the fused result provides a strong basic estimate for the second phase to operate on and enhance the despeckling performance. Output of the first phase competes with many standalone filters but failed to surpass the hybrid filters especially SAR-BM3D in terms of speckle suppression. Tab. 1 below provides a

comparison of the first phase with contemporary standalone filters i.e., NLM, WT and CT, and hybrid filters i.e., PPB, FANS and SAR-BM3D, in terms of PSNR and SSIM.

Table 1: Comparison of First Phase with Existing Filters on Cameraman at Speckle 0.03

	Noisy	NLM	WT	CT	PPB	FANS	SAR-BM3D	First Phase
PSNR	20.866	29.536	26.576	29.490	28.766	22.823	31.596	27.810
SSIM	0.282	0.304	0.311	0.455	0.255	0.405	0.379	0.443

2.2 Second Phase

The second phase computes a unique sequence of some predefined noise suppressing filters i.e., SRAD, wiener, wavelet, NLM, and edge preserving filters such as NLM based GF, wavelet based GF and curvelet based GF. This unique sequence is applied to the output of the first phase for enhancing its depeckling accuracy. In order to determine the unique sequence of the above mentioned filters, this study has explored the use of a multi objective optimization algorithm namely cuckoo search optimization (CSO) algorithm with PSNR, SSIM, and standard deviation (SD) as its objective function [24].

For our despeckling problem, the modified cuckoo search algorithm starts with an initial population of 5 nests holding one egg each (one sequence of 4 filters). The best eggs (solutions) are kept after evaluating their fitness through the objective function (PSNR & SSIM), and passed over to the next generations for quicker convergence. Remaining nests are populated using the levy distribution and their fitness is again compared with the best nests through the objective function [25]. Bad nests with poor performances are destroyed with the probability of 0.35. In order to determine the best combination of filters for despeckling each input image, the CSO iteratively maximizes PSNR and SSIM, and minimizes SD. In this experiment, the algorithm will stop after 30 iterations as it starts repeating values after 30 iterations.

The optimal sequence generated by the CSO comprises of four filters. Two of which gets fused i.e. one noise suppressing and edge preserving filter are combined to merge the information from two despeckled images. Position of the remaining two are adjusted in accordance with the fusion result to enhance the performance of the second phase. The CSO finds out which filters should be fused and which ones should be applied in a sequence before or after the fusion. The possible filter organizations are listed below:

Unlike some previous attempts, the second phase of the proposed filter does not consider SAR-BM3D as one of the candidate filter due to its high computational cost. The filter selection criteria for designing the second phase of the proposed filter includes minimal computational cost and capability to maximally suppress noise and preserve image edges. This criteria automatically redirects the filter selection decision towards the standalone filters as hybrid filters are costly. The selected filters are provided in Tab. 2 along with their used parameters.

The generated optimal sequences i.e., [1, (9, 11), 6] represent the number of filters. Thus, according to the sequence, [1, (31, 2), 7], the filters that would be applied to despeckle an image are: WT on the noisy image, Fusion of wiener and NLM based GF, and SRAD.

To justify the need of a sequential application of multiple filters, a Lena image corrupted with 0.03 simulated speckle is taken as an example. The visual comparison is also provided for better understanding of the proposed approach (Fig. 6).

Table 2: Detail of noise suppressing and edge preservation filters

Filter # in CSO design	Name of filter	Parameters
1,2	Wavelet Transform	Sym4 with denoising method Bayes and thresholding method median posteriori, wavelet with wiener filtering
3,4,5	Weiner filter	Mask = 3×3, 5×5, 7×7
6	NLM	Neighbor window size = 3, search window size = 21
7	SRAD Filter	Number_Of_Iterations = 15 and time stamp = 0.012
8	Original GF	Guidance image = Noisy image
9	GF based on WT and CT	Guidance image = Denoised image obtained after WT and CT in sequence
10	GF based on Curvelet Transform	Guidance image = Denoised image after CT
11	GF based on wavelets	Guidance image = Denoised image after WT
12	GF based on NLM	Guidance image = Denoised image after NLM

Figure 6: Result of applying combination (1, (12, 1), 6) on lena image corrupted with speckle 0.03

Fig. 6 shows the PSNR values after each step. Observation from Fig. 6 reveals that the PSNR value is at its maximum after applying the last filter. These initial results demonstrated the concept of adaptive computation which helps maintain image structures while performing the speckle suppression. A detailed comparison of hybrid despeckling filters i.e. PPB, FANS, SAR_BM3D and the proposed approach has been carried out on two test images i.e., boat and baboon. To prove the effectiveness of the proposed approach in terms of PSNR (Figs. 7 and 8) and SSIM (Figs. 9 and 10), this experiment has been conducted at several noise intensities. The CSO generates different sequences of filters for both images because of their dissimilar nature. This behavior of CSO demonstrates the adaptive nature of the proposed hybrid filter.

The image baboon is an indoor single object image containing less details as compared to the outdoor boat image. Hence, the permutation of filters generated by the CSO for baboon image is same at various noise intensities whereas different for boat image at different noise intensities (Tab. 3).
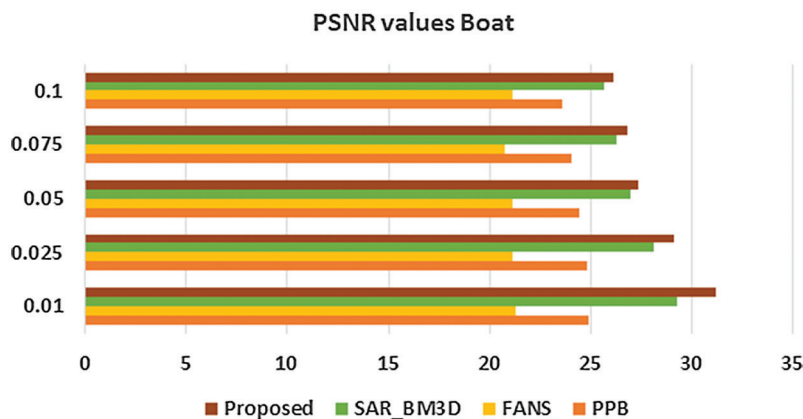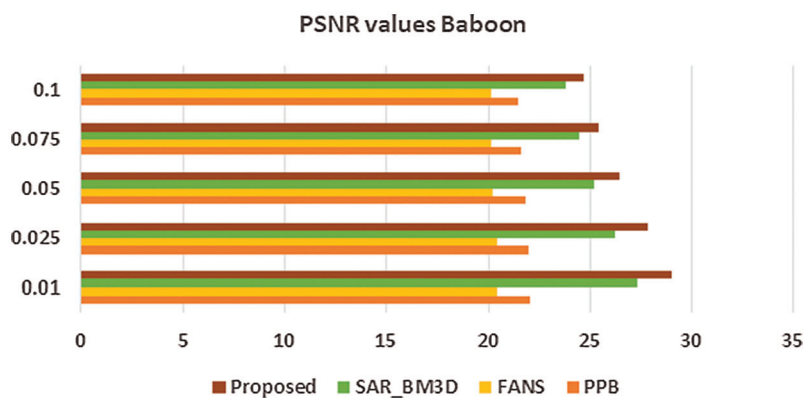
PSNR values Boat

Figure 7: PSNR values of boat image

PSNR values Baboon

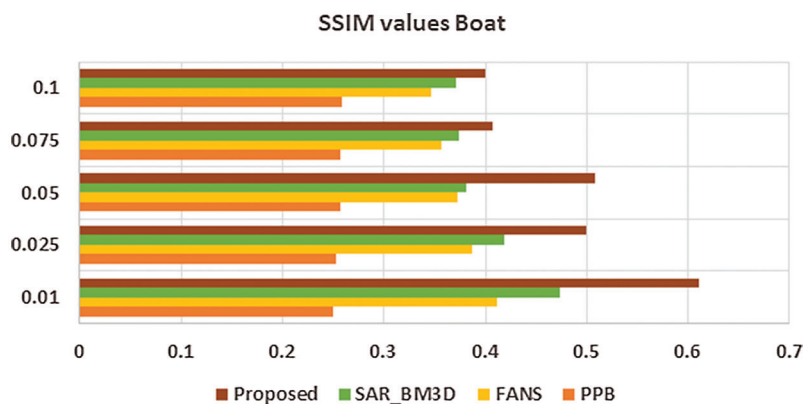**Figure 8:** PSNR values of baboon image

SSIM values Boat

Figure 9: SSIM values of boat image

3 Experimental Results on Standard Images

To investigate the strengths and weaknesses of the proposed filter, we first carried out an experiment on standard test images which are provided in Fig. 11. The selected gray scale test images are of different resolutions i.e., 256 × 256 and 512 × 512, and of different characteristics i.e., single and multi-object. Single object images i.e., Lena, baboon and Zelda, contain less details whereas indoor multi object

images such as fruits, peppers, man and living room, and outdoor multi object images i.e., boat and hill are rich in texture and edges. Filters that are used in this experiment for comparison include NLM, PPB, FANS, SAR-BM3D, Curvelets and Wavelets. After confirming the despeckling performance of the proposed filter on standard images, a satellite data set was used to demonstrate its robustness.
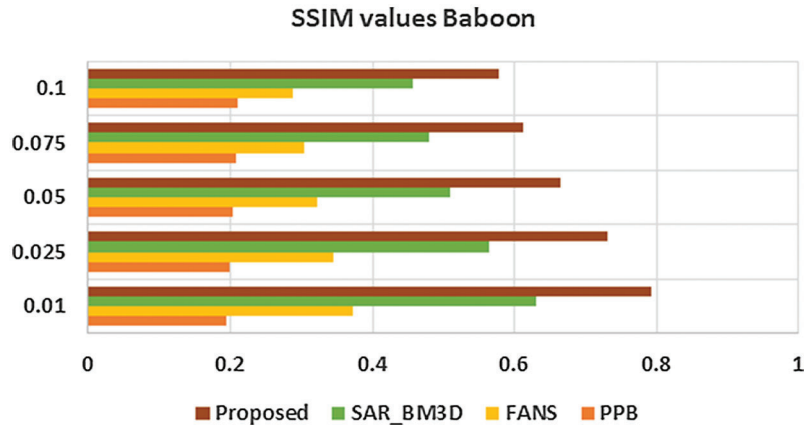

Figure 10: SSIM values of baboon image

Table 3: Permutation of filters for Baboon and Boat images

Image	0.01	0.025	0.05	0.075	0.1
Baboon	1,(6,12),6				
Boat	3,1,(6,12)	3,(1,12),7	9,(12,6),1	9,(6,12),6	9,6,(12,7)

Tabs. 4 and 5 below presents the despeckling results in terms of PSNR at simulated speckle with variance σ = 0.03 and σ = 0.05. The purpose of selecting two variance levels is to examine the performance of all filters at lower and higher levels of noise. Tabs. 6 and 7 presents the structure related information in terms of SSIM values. Despeckling results shown by the proposed filter on both types of images at several noise variances revealed its remarkable performance when compared with existing filters.

The proposed hybrid filter has shown an increase in PSNR values on all test images when compared with the standalone filters. Whereas, the curvelet transform has the best structure preserving capability as compared to the hybrid filters as depicted in Tabs. 5 and 7. The red highlighted values are greater than the proposed filter while yellow highlighted values are only greater than the SAR-BM3D. Mostly, curvelets perform better than the proposed filter in terms of SSIM, however, an exceptional behavior of NLM and wavelets has also been observed on the baboon and boat image.

The proposed filter has also demonstrated the good despeckling performance when assessed against the hybrid filters. It outperformed the present hybrid filters in terms of PSNR on all test images except the cameraman image. SAR-BM3D performs better despeckling on the cameraman image at both noise levels than the proposed. However, the proposed filter has shown the second good PSNR values at the cameraman image and it outperformed the SAR-BM3D in structural similarity index. The despeckling performance of the proposed filter on remaining test images, belonging to the discussed three categories, is remarkable.
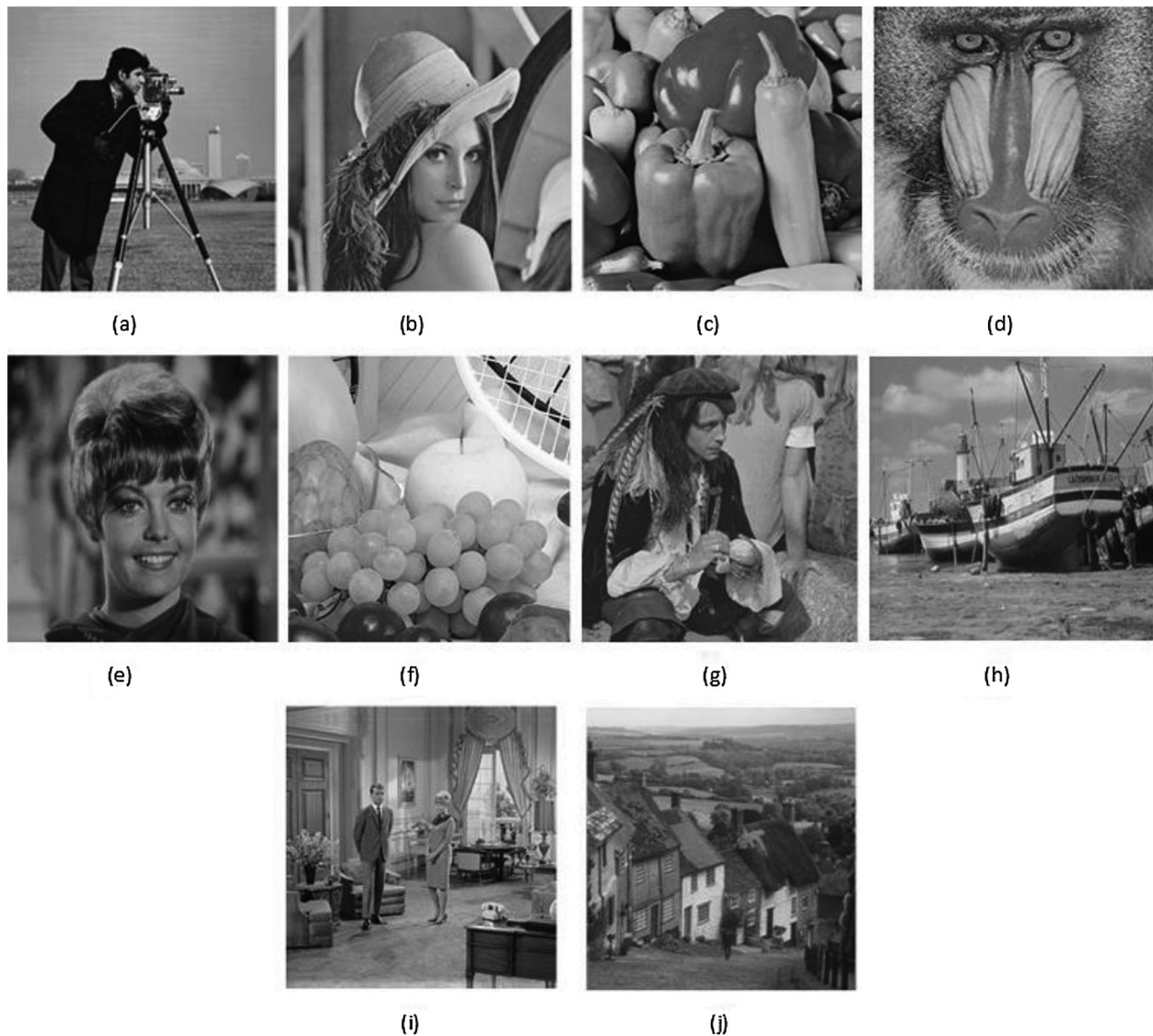
Figure 11: Standard test images. (a) Cameraman (512 × 512), (b) Lena (256 × 256), (c) Peppers (512 × 512), (d) Baboon (512 × 512), (e) Zelda (512 × 512), (f) Fruits (512 × 512), (g) Man (512 × 512), (h) Boat (512 × 512), (i) Living room (512 × 512), (j) Hill (512 × 512)

An increase of 0.5 and greater has been seen in PSNR values of Lena and Baboon at both noise intensities (Fig. 12). However, Zelda has shown an increase of 0.3 to 0.5. The SSIM values, instead, are increased to 0.8 and higher on all single object images (Fig. 13). The filter sequences for Lena and baboon images are same on two different noise intensities. Whereas, different permutations for Zelda has produced the said results.

Multi object indoor and outdoor images presented an increase in PSNR and SSIM values depicting better performance of the proposed hybrid filter. Two best results among the test images are the Man image at σ = 0.03 showing an increase of 0.8 in PSNR and the Peppers image with an increase of 0.8 at σ = 0.05. Moreover, the increase in SSIM values observed for both these categories ranging from 0.02 to 0.1. A visual comparison of a multi object image is also provided below for further comprehension of the robustness of the proposed filter (Fig. 14).

Table 4: PSNR values of existing and proposed filter at speckle 0.03

Image	Noisy	NLM	Curvelets	Wavelets	FANS	PPB	SARBM-3D	Proposed	Proposed Sequence
Cameraman	20.866	29.536	29.490	26.576	22.823	28.766	31.596	31.251	[7,(3,12),1]
Lena	20.961	27.493	26.565	26.147	21.722	25.046	27.609	**28.077**	[1,(12,1),6]
Peppers	21.020	29.266	28.522	27.227	22.732	27.392	30.503	**30.669**	[9,(12,2),6]
Baboon	20.784	25.879	26.578	26.245	20.436	21.938	25.962	**27.449**	[1,6,(12,6)]
Zelda	23.380	31.017	32.092	29.371	25.034	30.049	33.415	**33.721**	[9,(12,2),7]
Fruits	19.121	28.427	27.014	27.357	20.604	26.839	28.765	**29.329**	[9,1,(12,6)]
Man	21.717	27.695	28.301	26.548	21.920	25.402	28.273	**29.139**	[9,(12,1),6]
Boat	20.647	27.871	27.305	26.805	20.427	24.694	27.828	**28.673**	[3,1,(12,7)]
Living Room	21.219	27.421	27.309	26.635	21.966	24.238	28.134	**28.451**	[11,(12,6),1]
Hill	21.884	27.402	28.411	26.862	22.129	25.431	28.942	**29.215**	[9,1,(12,6)]

Table 5: PSNR values of existing and proposed filter at speckle 0.05

Image	Noisy	NLM	Curvelets	Wavelets	FANS	PPB	SAR-BM3D	Proposed	Proposed sequence
Cameraman	18.673	28.139	28.104	24.585	22.842	28.128	30.245	30.191	[7,(12,2),6]
Lena	18.851	26.157	25.809	24.891	21.721	24.787	26.790	**27.378**	[1,(12,1),6]
Peppers	18.869	27.951	27.405	25.557	22.733	27.085	29.366	**30.121**	[9,(12,2),6]
Baboon	18.581	24.377	25.867	24.664	20.374	21.802	25.118	**26.006**	[1,(6,12),6]
Zelda	21.154	29.496	30.783	27.450	25.118	29.606	32.108	**32.683**	[9,(12,2),7]
Fruits	17.079	26.912	25.531	25.946	21.273	26.241	27.491	**27.749**	[9,6,(12,6)]
Man	19.539	26.594	27.399	25.097	22.476	25.199	27.505	**28.119**	[(7,9).6,1]
Boat	18.465	26.571	26.384	25.532	21.511	24.436	27.013	**27.73**	[9,(12,6),1]
Living room	19.030	26.013	26.478	25.416	21.930	24.052	27.322	**27.391**	[9,(12,7),1]
Hill	19.773	26.264	27.422	25.480	23.018	25.166	28.114	**28.265**	[9,(12,7),6]

Table 6: SSIM values of existing and proposed filter at speckle 0.03

Images	Noisy	NLM	Curvelets	Wavelets	FANS	PPB	SAR-BM3D	Proposed
Cameraman	0.282	0.304	0.455	0.311	0.405	0.255	0.379	**0.407**
Lena	0.385	0.484	0.510	0.469	0.459	0.385	0.506	**0.537**
Peppers	0.302	0.403	0.447	0.369	0.439	0.352	0.431	**0.459**
Baboon	0.485	0.553	0.674	0.642	0.340	0.200	0.548	**0.632**
Zelda	0.307	0.504	0.561	0.478	0.568	0.469	0.578	**0.597**
Fruits	0.174	0.300	0.334	0.285	0.293	0.237	0.331	**0.365**

Table 6 (continued).

Images	Noisy	NLM	Curvelets	Wavelets	FANS	PPB	SAR-BM3D	Proposed
Man	0.372	0.457	0.562	0.458	0.397	0.278	0.461	**0.535**
Boat	0.344	0.446	0.507	0.411	0.384	0.253	0.407	**0.518**
Living Room	0.395	0.481	0.551	0.465	0.421	0.264	0.501	**0.533**
Hill	0.397	0.430	0.561	0.434	0.427	0.244	0.463	**0.507**

Table 7: SSIM values of existing and proposed filter at speckle 0.05

Images	Noisy	NLM	Curvelets	Wavelets	FANS	PPB	SAR-BM3D	Proposed
Cameraman	0.235	0.269	0.418	0.267	0.384	0.256	0.354	**0.376**
Lena	0.322	0.430	0.473	0.410	0.445	0.382	0.472	**0.494**
Peppers	0.244	0.365	0.405	0.329	0.423	0.354	0.410	**0.444**
Baboon	0.397	0.455	0.630	0.538	0.321	0.203	0.507	**0.665**
Zelda	0.239	0.453	0.509	0.427	0.544	0.472	0.554	**0.566**
Fruits	0.136	0.251	0.287	0.241	0.274	0.231	0.290	**0.325**
Man	0.298	0.398	0.514	0.389	0.380	0.282	0.427	**0.493**
Boat	0.278	0.388	0.467	0.366	0.367	0.255	0.379	**0.439**
Living room	0.323	0.413	0.509	0.398	0.402	0.268	0.475	**0.499**
Hill	0.312	0.369	0.522	0.368	0.407	0.244	0.435	**0.481**
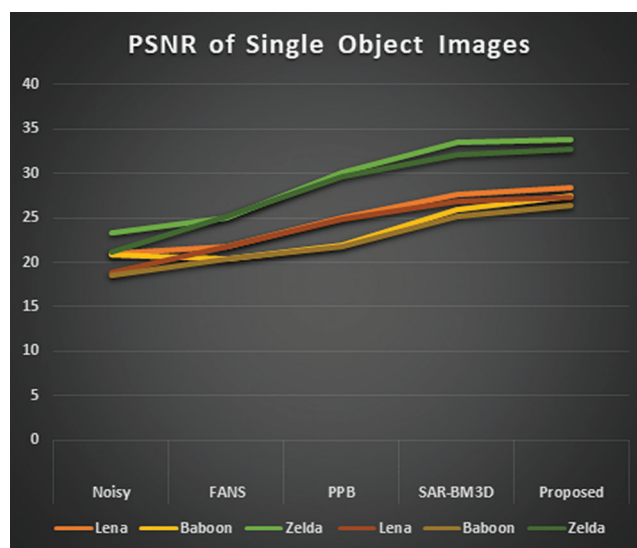
Figure 12: PSNR values at σ = 0.03 and σ = 0.05

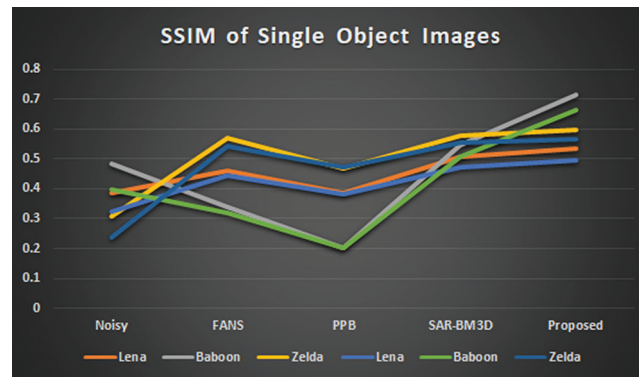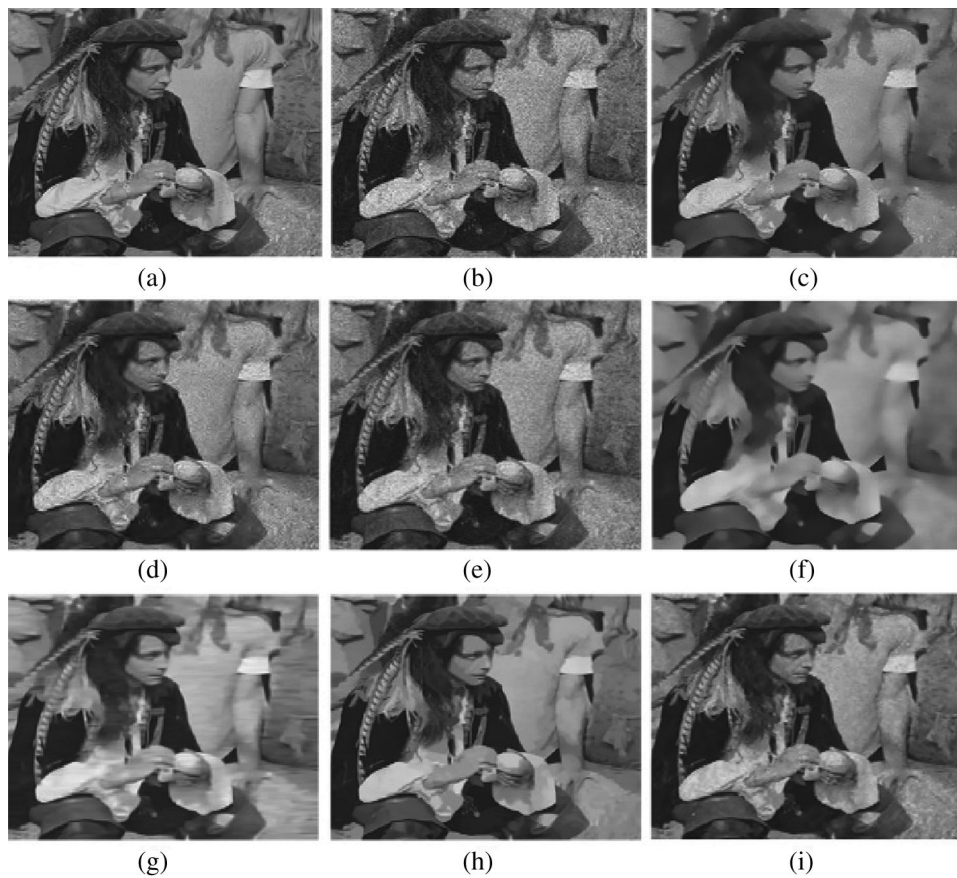**Figure 13:** SSIM values at σ = 0.03 and σ = 0.05

Figure 14: Man at 0.05. (a) Original, (b) Noisy, (c) NLM, (d) WT, (e) CT, (f) PPB, (g) FANS, (h) SARBM3D, (i) Proposed

Poor noise suppression has been shown by both wavelets and curvelets. However, the curvelet transform tends to preserve the structural similarity in many images better than the SARBM3D. NLM also failed to preserve the structure of images but showed better noise suppression due to the blurring of image details. PPB has done the maximum over smoothing compared to the others and did not perform well in terms of both PSNR and SSIM on all images. Similarly, FANS also failed to accomplish the results equivalent to

that of SAR-BM3D although it claimed the ability of detail preservation. The despeckling behavior of SAR-BM3D can be analyzed from Fig. 14 provided above. SAR-BM3D attempted to minimize the MMSE by blurring the image details. Extra whitening on Man's face and hands and on the first lady's shirt, the disappearance of texture on second lady's shirt are the problems of over smoothing caused by SAR-BM3D. On the other hand, the proposed filter suppresses noise without these effects.

A histogram analysis of the image peppers is provided below as an evidence that the proposed filter restores speckled images even better than the various existing hybrid filters (Fig. 15).
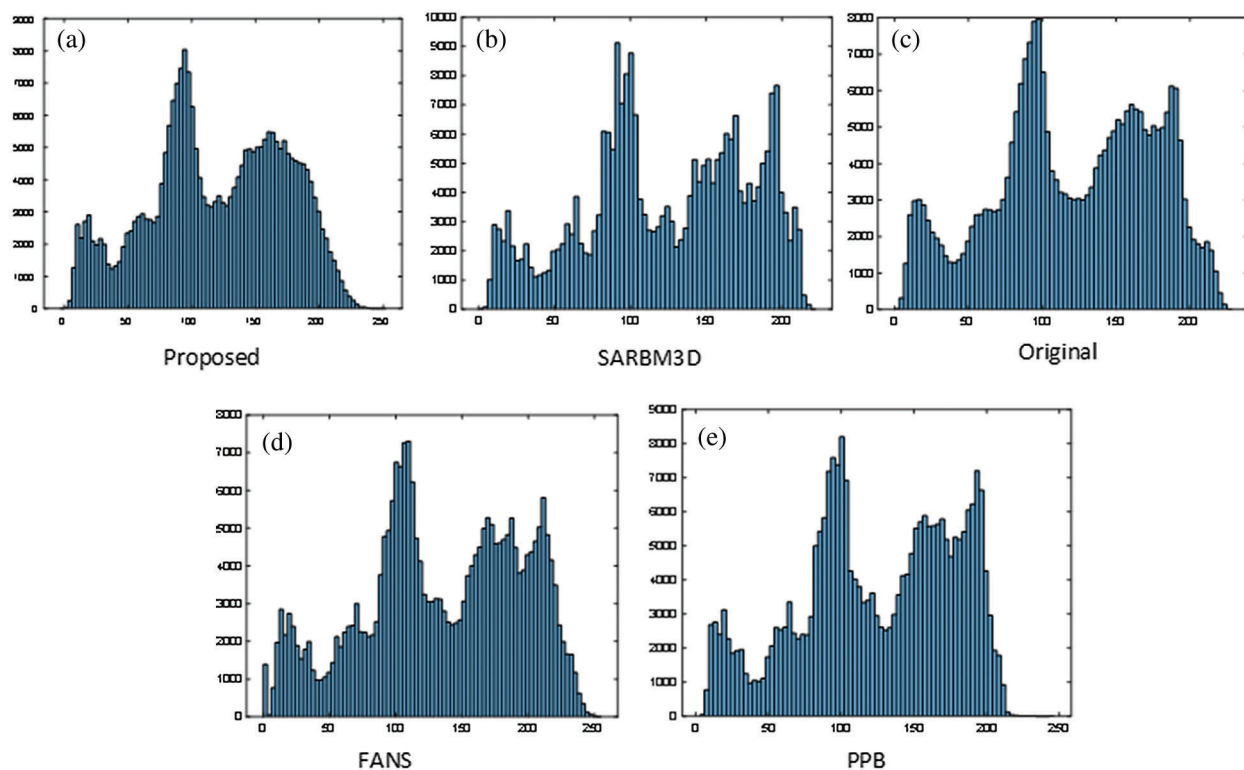

Figure 15: Comparison of Hybrid filters for Peppers at 0.03. (a) Proposed, (b) SAR-BM3D, (c) Original, (d) FANS, (e) PPB

4 Experimental Results on SAR Imagery

Performance of the proposed approach is also assessed on real SAR imagery. For this experiment, we extracted two patches of 256 × 256 from single look Terra-SAR-X images which are provided in Fig. 16 below. ENL values of the existing and the proposed algorithm after despeckling different regions of interest (ROI) are provided in Tab. 8.

As speckle is inherent in SAR images, it is not possible to obtain clean SAR images and thus we can't use PSNR and SSIM as the objective function of CSO. So, we propose standard deviation (SD) of SAR images as the objective function of CSO when we have to deal with real SAR imagery. The sequence determined by the CSO for first SAR image is [7, (1,12), 9] while [7, (9,1), 9] is for the second image.

Tab. 8 presents the ENL values of four regions of interests. ROI1 and ROI2 are taken from image1 while ROI3 and ROI4 belongs to the image2. Higher ENL values are shown by the PPB filter which does maximum smoothing of details as compared to all other standalone and hybrid filters. FANS and PPB

both performs over smoothening, so their ENL values are greater than the others. Then comes SAR-BM3D, as it also blurs some of the details due to wiener filtering. The proposed filter did not surpass hybrid filters in smoothening of homogeneous regions as it is an edge preserving filter. And being its focus on preserving edges, it does not over smoothens details which ultimately results in lower ENL values.
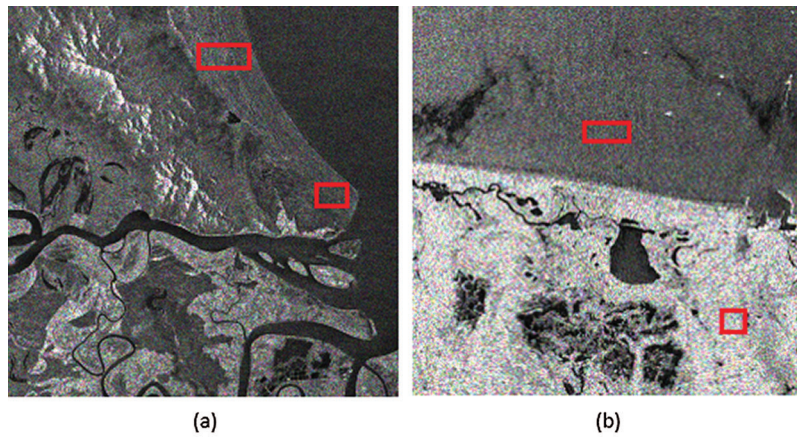

(a)   (b)

Figure 16: (a) Image 1, (b) Image 2

Table 8: ENL Values of existing and proposed filter

	Noisy	NLM	Curvelets	Wavelets	FANS	PPB	SAR-BM3D	Proposed
ROI1	11.315	91.339	70.621	55.892	153.623	**206.014**	118.294	114.511
ROI2	22.889	121	135	66	432	**935**	314	151
ROI3	65.735	128.7	93.95	101.50	4253	**5342.4**	1595.6	540.23
ROI4	43.936	80.42	75.76	67.23	585	**1290.1**	802.76	86.643

All the empirical evaluations on standard and real SAR imagery are provided in Tabs. 4–7 which clearly shows the outstanding performance of the proposed hybrid filter in terms of PSNR and SSIM except on the cameraman image. However, the ENL values are lower than the other hybrid filters. One of the reasons for lower ENLs may be the despeckling without causing any kind of blurs. This behavior eventually helps in proving the best edge preservation capability of the proposed filter. The sequences generated by the CSO for despeckling of each image are also provided in the tables which may or may not be the same for any image at different noise intensities. This adaptive nature of the proposed hybrid filter is definitely the result of employing CSO in its design. Figs. 14 and 15 presents the noise suppression capability of the proposed on standard images whereas in Fig. 17, visual comparison of a real SAR image is provided. Robustness and effectiveness of the proposed filter can be analyzed through provided tables and figures.
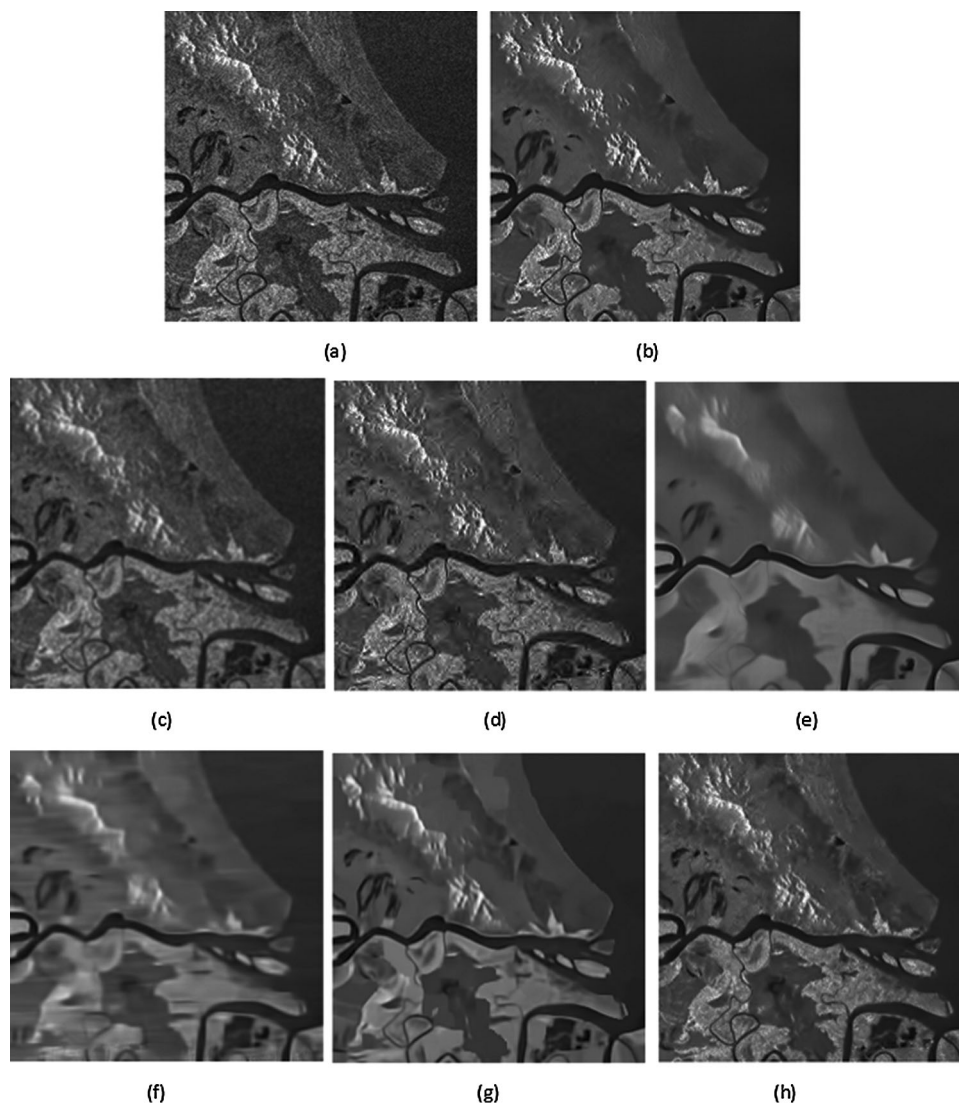
Figure 17: Performance comparison of filters (a) Noisy, (b) NLM, (c) WT, (d) CT, (e) PPB, (f) FANS, (g) SARBM3D, (h) Proposed

5 Conclusion

To tackle the issue of speckle suppression while feature preservation, this study proposes a two phase hybrid filter. The first phase help preserve edges with a new edge detection criterion presented for the guided filter. The first phase also combines the output of the GF with the wiener filter for adequate smoothing. The result of the first phase is considered as an initial despeckled estimate and passed on to the second phase for further enhancement. The second phase determines optimal sequences of some predefined speckle suppressing and edge preserving filters with the help of CSO. Therefore, the second phase is helpful in boosting the despeckling accuracy while preserving edges.

We have utilized the standard test and real SAR images to assess the despeckling performance of the proposed and state-of-the-art filters in terms of PSNR, SSIM and ENL. The empirical evaluation revealed that the generated sequences of filters are in accordance with the image and noise characteristics. And this adaptive nature of the proposed filter helps in obtaining better despeckling accuracy and structural

similarity on different noise levels and types of images. Hence, the despeckled images produced by the proposed hybrid filter can be used in many automated image processing applications.

Conflicts of Interest: The authors declare that they have no conflicts of interests.

References
[1]   A. Moreira, P. Prats-Iraola, M. Younis, G. Krieger, I. Hajnsek *et al.,* "A tutorial on synthetic aperture radar," *IEEE Geoscience and Remote Sensing Magazine*, vol. 1, no. 1, pp. 6–43, 2013.

[2]   F. Argenti, A. Lapini, T. Bianchi and L. Alparone, "A Tutorial on speckle reduction in synthetic aperture radar images," *IEEE Geoscience and Remote Sensing Magazine*, vol. 1, no. 3, pp. 6–35, 2013.

[3]   M. Malik, F. Ahsan and S. Mohsin, "Adaptive image denoising using cuckoo algorithm," *Soft Computing*, vol. 20, no. 3, pp. 925–938, 2014.

[4]   D. Devapal, S. Kumar and C. Jojy, "Comprehensive survey on SAR image despeckling techniques," *Indian Journal of Science and Technology*, vol. 8, no. 24, pp. 1–4, 2015.

[5]   A. Buades, B. Coll and J. Morel, "A review of image denoising algorithms, with a new one," *Multiscale Modeling & Simulation*, vol. 4, no. 2, pp. 490–530, 2005.

[6]   B. K. Shreyamsha Kumar, "Image denoising based on non local-means filter and its method noise thresholding," *Signal Image and Video Processing*, vol. 7, no. 11, pp. 1211–1227, 2013.

[7]   J. Strack, E. J. Candes and D. L. Donoho, "The Curvelet transform for image denoising," *IEEE Transactions On Image Processing*, vol. 11, no. 6, pp. 670–684, 2002.

[8]   W. Ni and X. Gao, "Despeckling of SAR image using generalized guided filter with bayesian nonlocal means," *IEEE Transactions on Geoscience and Remote Sensing*, vol. 54, no. 1, pp. 567–579, 2016.

[9]   Y. Y. Li, H. Gong, D. Fang and Y. Zhang, "An Adaptive method of speckle reduction and feature enhancement for SAR images based on Curvelet transform and particle swarm optimization," *IEEE Transactions On Geoscience And Remote Sensing*, vol. 49, no. 8, pp. 3105– 3116, 2011.

[10] F. Zakeri and M. J. Valadan, "Adaptive method of speckle reduction based on curvelet transform and thresholding neural network in synthetic aperture radar images," *Journal of Applied Remote Sensing*, vol. 9, no. 1, pp. 1–11, 2015.

[11] W. Wang, X. Zhang and X. Wang, "Speckle suppression method in SAR image based on Curvelet domain BivaShrink model," *Journal of Software*, vol. 8, no. 4, pp. 947–954, 2013.

[12] K. Dabov, A. Foi, V. Katkovnik and K. Egiazarian, "Image denoising by sparse 3-D Transform-Domain collaborative filtering," *IEEE Transactions on Image Processing*, vol. 16, no. 8, pp. 2080–2095, 2007.

[13] S. Parrilli, M. Poderico, C. Angelino and L. Verdoliva, "A Nonlocal SAR image denoising algorithm based on LLMMSE wavelet shrinkage," *IEEE Transactions on Geoscience and Remote Sensing*, vol. 50, no. 2, pp. 606–616, Feb. 2012.

[14] D. Cozzolino, S. Parrilli, G. Scarpa, G. Poggi and L. Verdoliva, "Fast adaptive nonlocal SAR despeckling," *IEEE Geoscience and Remote Sensing Letters*, vol. 11, no. 2, pp. 524–528, 2014.

[15] C. Deledalle, L. Denis, G. Poggi, F. Tupin and L. Verdoliva, "Exploiting patch similarity for SAR image processing: The nonlocal paradigm," *IEEE Signal Processing Magazine*, vol. 31, no. 4, pp. 69–78, 2014.

[16] Linlin Xu, J. Li Yuanming Shu and Junhuan Peng, "SAR image denoising via clustering-based principal component analysis," *IEEE Transactions on Geoscience and Remote Sensing*, vol. 52, no. 11, pp. 6858–6869, 2014.

[17] D. Xu and Y. Tian, "A Comprehensive survey of clustering algorithms," *Annals of Data Science*, vol. 2, no. 2, pp. 165–193, 2015.

[18] D. Gragnaniello, G. Poggi and L. Verdoliva, "Classification based nonlocal SAR despeckling," in *Proc. Tyrrhenian Workshop on Advances in Radar and Remote Sensing*, pp. 121–125, 2012.

[19] D. Gragnaniello, G. Poggi, G. Scarpa and L. Verdoliva, "SAR image despeckling by soft classification," *IEEE Journal of Selected Topics in Applied Earth Observations and Remote Sensing*, vol. 9, no. 6, pp. 2118–2130, 2016.

[20] L. Verdoliva, R. Gaetano, G. Ruello and G. Poggi, "Optical-driven nonlocal SAR despeckling," *IEEE Geoscience and Remote Sensing Letters*, vol. 12, no. 2, pp. 314–318, 2015.

[21] H. Chio and J. Jeong, "Speckle noise reduction technique for SAR images using statistical characteristics of speckle noise and discrete wavelet transform," *Remote Sensing*, vol. 11, no. 10, pp. 1184, 2019.

[22] H. Salehi, J. Vahidi, T. Abdeljawad, A. Khan and S. Y. Bozorgi Rad, "A SAR image despeckling method based on an extended adaptive wiener filter and extended guided filter," *Remote Sensing*, vol. 12, no. 15, pp. 2371, 2020.

[23] K. He, J. Sun and X. Tang, "Guided image filtering," *IEEE Transactions on Pattern Analysis and Machine Intelligence*, vol. 35, no. 6, pp. 1397–1409, 2013.

[24] X. S. Yang and S. Deb, "Cuckoo search: Recent advances and applications," *Neural Computing and Applications*, vol. 24, no. 1, pp. 169–174, 2014.

[25] X. S. Yang, "Engineering optimisation: An introduction with metaheuristic applications, John Wiley and Sons, 2010. [Online]. Available at: https://www.amazon.com/Engineering-Optimization-Introduction-Metaheuristic-Applications/dp/0470582464.